

Gas-Phase Conformational Analysis of 1,4,7-Trithiacyclononane

Brian J. Drouin, Nadine E. Gruhn,[†] John F. Madden, Stephen G. Kukolich, Michael Barfield,* and Richard S. Glass

Department of Chemistry, The University of Arizona, P.O. Box 210041, Tucson, Arizona 85721

Received: August 4, 1997[⊗]

Conformational analysis of 1,4,7-trithiacyclononane, [9]aneS₃, in the gas phase was done using three techniques: ab initio molecular orbital calculations at the HF and MP2 levels as well as microwave and photoelectron spectroscopies. The photoelectron spectroscopic data show evidence for at least two conformations with different ionization energies. Using the calculated photoelectron spectra, the observed sulfur 3p ionization peaks can be assigned to C₁ and C₂ conformations. Forty of the observed microwave transitions can be assigned to a C₁ symmetry, asymmetric top, rigid rotor spectrum with rotational constants A = 1155.651(3) MHz, B = 998.442(3) MHz, and C = 629.426(2) MHz. Additional microwave lines are believed to be due to a nonrigid C₂ symmetry conformation. No significant populations of conformers of higher symmetry are found.

Introduction

1,4,7-Trithiacyclononane, [9]aneS₃, shows a remarkable ability to coordinate metal ions.^{1,2} Typically it functions as a tridentate ligand adopting a geometry comparable to that determined in the solid state by X-ray crystallographic methods.³ Furthermore, the gas-phase photoelectron (PES) spectrum of [9]aneS₃ was interpreted in terms of this conformation because of the large splitting of the sulfur 3p lone pair ionization and their 2:1 ratio.^{4–6} Consequently, it was suggested that the preferential adoption of the [333] conformation (C₃ symmetry) with the sulfur atoms endodentate rendered this ligand preorganized for tridentate coordination.⁷

Subsequent studies have demonstrated the remarkable flexibility of [9]aneS₃ in its coordination complexes.⁸ For example, the [1222] conformation (with approximate C₂ symmetry) occurs both as the monodentate ligand in Au^I ([9]aneS₃)₂⁹ and in bridging the two copper atoms in the Cu₂^I ([9]aneS₃)₃ complex.¹⁰ A different conformation is found in Cu^I ([9]aneS₃)₂.¹¹ Furthermore, a gas-phase electron diffraction (GED) study¹² of [9]aneS₃ found that the structures with C₁ and C₂ symmetry fit the data better than the solid-state C₃ conformation, and the best agreement was with the C₁ structure. It is worth noting that this GED study was done at a higher temperature than the PES study which could result in differences in conformational populations. The observation of a singlet in the ¹H NMR spectrum of [9]aneS₃ suggested¹³ that there are conformational changes that are rapid on the NMR time scale. Dynamic analysis of this process showed correlated g⁺ → g⁻ transitions about the three gauche C–C bonds of the [333] conformer and a multiplicity of available structures. Variable temperature Raman and infrared spectroscopic studies¹⁴ indicated that the predominant liquid conformation is different from that in the solid. Computational results⁴ based on molecular mechanics and semiempirical methods suggested that the C₂ conformer is more stable than the C₃ conformer. Subsequently, MM2 calculations showed a C₁ conformer to be slightly lower in energy than the C₃ conformer.¹² A recent conformational search found 13 different conformations within 4 kcal/mol of the lowest energy (presumed C₃) conformer.⁸

As a result of the controversy concerning the conformation of [9]aneS₃ in the gas phase and in solution, this system was reinvestigated using ab initio computational methods as well as photoelectron and microwave spectroscopies. The results reported here provide new insights into the conformation of [9]aneS₃ in the gas phase.

Theoretical Calculations

All molecular geometries are fully optimized using the Gaussian 94 codes¹⁵ both at the Hartree–Fock and MP2 levels of Møller–Plesset¹⁶ perturbation theory with split-valence basis sets and polarization functions¹⁷ on all non-hydrogen elements (6-31G*). The frozen core approximation was used for MP2 calculations wherein the inner-shell electrons of the carbon and sulfur atoms were not included in the calculations of electron correlation energies. All computations were performed using RISC 6000 IBM590 workstations.

Experimental Section

Purification of [9]aneS₃. The sample of 1,4,7-trithiacyclononane was purchased from Aldrich Chemical Co. and further purified via preparative thin-layer chromatography (TLC) followed by recrystallization from pentane and sublimation. The TLC was performed twice using a 1:1 mixture of hexanes and dichloromethane as eluent (R_f = 0.4 hexane:CH₂Cl₂ 1:3). The crystals recovered from the pentane were dried over P₂O₅ overnight and sublimed.

Photoelectron Spectroscopy. The He I photoelectron spectra were recorded using a McPherson ESCA36 instrument that features a 36 cm hemispherical analyzer (8 cm gap) and custom designed sample cells and detection and control electronics.^{18–20} The argon ²P_{3/2} ionization at 15.759 eV was used as an internal calibration lock of the absolute ionization energy. The difference between the argon ²P_{3/2} and the methyl iodide ²E_{1/2} ionization at 9.538 eV was used to calibrate the ionization energy scale. During collection the instrument resolution (measured using fwhm of the argon ²P_{3/2} peak) was 0.014–0.022 eV. All data are intensity corrected with an instrument analyzer sensitivity function which was experimentally determined. The He I spectra were corrected for the He I β line ionizations. This correction is necessary because discharge sources are not monochromatic.²¹

[†] Center for Gas-Phase Photoelectron Spectroscopy, Department of Chemistry, The University of Arizona.

[⊗] Abstract published in *Advance ACS Abstracts*, November 15, 1997.

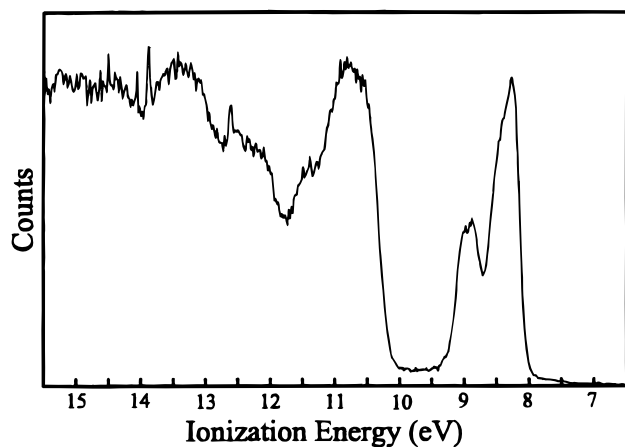


Figure 1. Experimental He I PES spectrum of [9]aneS₃.

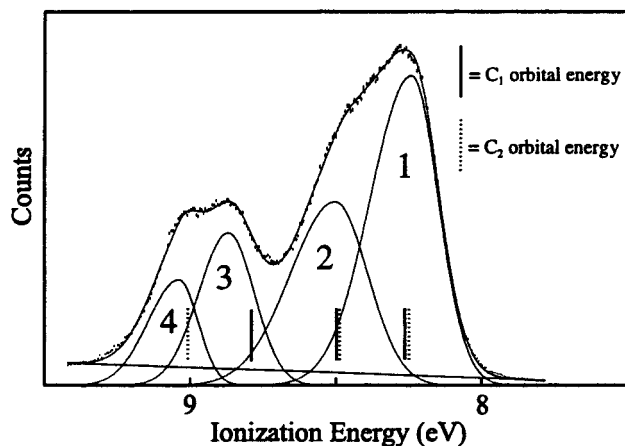


Figure 2. Expanded He I PES spectrum in the S lone-pair ionization region. The vertical lines represent the calculated orbital energies for conformations of C₁ and C₂ symmetries (see text for details). Table 1 shows that parameters obtained for the Gaussian peaks 1–4.

TABLE 1: Positions, Amplitudes and Peak Widths of the Gaussian Peaks Used to Fit the Experimental PES Spectra^a

peak no.	position (eV)	peak width		rel area
		high	low	
1	8.24	0.33	0.22	1.00
2	8.50	0.36	0.26	0.68
3	8.87	0.24	0.21	0.41
4	9.04	0.25	0.15	0.24

^a See Figure 2.

The sample sublimed cleanly with no detectable evidence of decomposition products in the gas phase or as a solid residue. Spectra were collected at a sublimation temperature (at 10⁻⁴ Torr) of 60 ± 2 °C, which was monitored using a “K” type thermocouple passed through a vacuum feedthrough and attached directly to the sample cell. The measured PES spectrum of [9]aneS₃ is shown in Figure 1.

In the expanded spectrum shown in Figure 2, the vertical length of each data mark represents the experimental variance of that point.²² The ionization bands are represented analytically with the best fit of asymmetric Gaussians. The Gaussians are defined with their position, amplitude, half-width for high binding energy side, and the half-width for low binding energy side, which are given in Table 1. The peak positions and half-widths are reproducible to about ±0.02 eV (~3σ level). The confidence limit for the relative Gaussian areas are about 5%, with the primary sources of uncertainty being the determination of the baseline subtracted from the bands due to electron scattering and fitting in the tails of the bands. If a Gaussian

TABLE 2: Measured and Calculated Transition Frequencies for the C₁ Conformation of [9]aneS₃; The Standard Deviation of the Fit Was 33 KHz

measd (MHz)	calcd (MHz)	diff (MHz)	rel int	quantum number
				J'K _a 'K _c ' / J _{K_aK_c}
5473.7536(12)	5473.750	0.0036	0.1	4 ₁₄ -3 ₁₃
5479.6011(04)	5479.598	0.0031	0.2	4 ₀₄ -3 ₀₃
5532.0722(45)	5532.065	0.0072	0.3	3 ₂₁ -2 ₂₀
6256.0043(07)	6255.992	0.0123	0.7	3 ₂₁ -2 ₁₁
6290.8840(02)	6290.881	0.0030	1.0	4 ₂₃ -3 ₂₂
6315.3604(33)	6315.344	0.0164	0.6	3 ₀₂ -2 ₀₂
6432.7524(20)	6432.748	0.0044	0.3	4 ₁₃ -3 ₁₂
6462.2807(30)	6462.278	0.0027	2.0	3 ₂₂ -2 ₁₂
6591.2537(56)	6591.250	0.0037	1.0	8 ₁₈ -8 ₁₇
6609.2199(24)	6609.213	0.0069	4.0	3 ₃₀ -2 ₂₀
6720.8432(13)	6720.833	0.0102	4.0	3 ₃₁ -2 ₂₁
6734.8092(16)	6734.695	0.1142	4.0	5 ₁₅ -4 ₁₄
6735.6294(05)	6735.748	-0.1186	4.0	5 ₀₅ -4 ₀₄
6811.1636(28)	6811.159	0.0074	3.0	4 ₃₂ -3 ₃₁
7256.4569(10)	7256.456	0.0009	0.5	3 ₂₁ -4 ₂₂
7328.2329(21)	7328.227	0.0059	0.8	4 ₃₁ -3 ₃₀
7603.0177(12)	7603.023	-0.0053	0.4	5 ₂₄ -4 ₂₃
7640.3710(07)	7640.375	-0.0040	0.6	5 ₁₄ -4 ₁₃
7993.8904(18)	7993.899	-0.0086	1.3	6 ₀₆ -5 ₀₅
7993.9900(13)	7994.002	-0.0120	1.8	6 ₁₃ -5 ₁₅
8329.5889(27)	8329.597	-0.0081	1.0	5 ₃₃ -4 ₃₂
8344.6523(36)	8344.648	0.0043	0.5	4 ₂₂ -3 ₁₂
8405.3753(27)	8405.376	-0.0007	0.2	4 ₃₁ -3 ₂₁
8512.9652(42)	8512.950	0.0152	1.0	4 ₁₃ -3 ₀₃
8551.7428(03)	8551.727	0.0158	0.6	4 ₂₃ -3 ₁₃
8648.3947(39)	8648.388	0.0067	0.8	4 ₃₂ -3 ₂₂
8653.4117(34)	8653.421	-0.0093	0.8	5 ₂₃ -4 ₂₂
8675.6497(29)	8675.655	-0.0053	0.5	5 ₄₂ -4 ₄₁
8874.4035(15)	8874.418	-0.0145	2.0	6 ₂₅ -5 ₂₄
8881.3564(34)	8881.370	-0.0136	2.5	6 ₁₅ -5 ₁₄
8921.0378(46)	8921.048	-0.0102	1.5	4 ₄₀ -3 ₃₀
9241.2041(24)	9241.221	-0.0169	0.4	5 ₃₂ -4 ₃₁
9252.7183(29)	9252.748	-0.0297	0.3	7 ₀₇ -6 ₀₆
9712.0377(09)	9712.050	-0.0123	0.2	6 ₃₄ -5 ₃₃
9840.2789(39)	9840.300	-0.0211	0.1	6 ₂₄ -5 ₂₃
10135.0193(52)	10135.050	-0.0307	0.5	7 ₂₆ -6 ₂₅
10390.1262(67)	10390.141	-0.0148	0.5	5 ₃₂ -4 ₂₂
10511.5192(09)	10511.560	-0.0408	0.2	8 ₀₈ -7 ₀₇

substantially overlaps another Gaussian, the total areas of the bands are known with the same confidence, but the individual Gaussian areas are not independent and are thus more uncertain. The number of peaks used in the fit was based solely on the features of the ionization bands. Fitting procedures are described in more detail elsewhere.²²

Microwave Spectroscopy. The microwave spectrum was scanned in the 6–11 GHz range using a Flygare-Balle type spectrometer system.²³ The sample and pulse valve (General Valve 9-181) were maintained at 70–90 °C to produce significant vapor pressure. The sample, mixed with neon at 0.6–1.0 atm, was pulsed into the Fabry–Perot microwave cavity for observation of the spectra. Measured frequencies are listed in Tables 2 and 3. The least-squares fit, calculated transition frequencies for “a” and “c” dipole transitions are also shown in Table 2. For a comparison of the predicted C₁ spectrum with the experimental spectrum, see Figure 4.

Results

Theoretical Studies. Ab initio MO calculations were performed for the five lowest energy conformations described by Beech et al.⁸ One of the structures (“c” in their notation) did not converge at the HF/6-31G* level but converged to the C₁ structure at the MP2/6-31G* level. Calculations of the vibrational frequencies were performed for the four conformers at the HF/6-31G* level. Since only real frequencies were obtained, it appears that all four represent minima in the

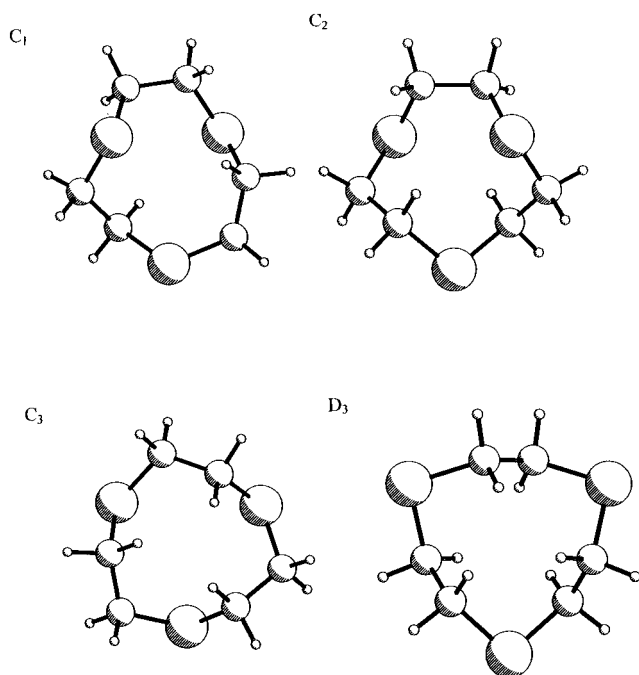


Figure 3. Plots of the four MP2 minimized conformations.

TABLE 3: Unassigned Measured Transitions in the Microwave Spectrum of [9]aneS₃

freq (MHz)	int	freq (MHz)	int
6360.8205(09)	1.5	6736.1397(26)	3.0
6462.3075(23)	2.0	6749.3582(49)	2.0
6472.7904(35)	1.5	6798.4589(19)	3.0
6477.7856(40)	0.5	6812.0183(17)	3.0
6482.8059(06)	2.5	6831.6640(28)	3.0
6482.8323(24)	2.5	6887.7214(37)	1.0
6632.5861(27)	2.0	8617.1207(15)	1.5
6668.6919(28)	3.0	8944.5579(24)	4.0
6677.3374(39)	2.0	9015.1831(35)	1.5
6677.9453(49)	2.0	9042.2083(17)	2.0
6696.1658(54)	2.5	9071.2643(18)	2.5

conformational energy hypersurface.²⁴ The bond lengths and bond angles (which were fully optimized at the MP2 level) associated with the non-hydrogen atoms are entered in Table 4 and the structures drawn in Figure 3. Only those obtained for the *C*₃ structure are consistent with the X-ray diffraction results shown in the first column of Table 4.

The calculated energies for the various conformers relative to the lowest energy structures are entered in Table 5. At the HF and MP2 levels the *C*₁ and *C*₂ conformers have the lowest energies. This is consistent with the results of Blom et al.¹² that showed either the *C*₁ or *C*₂ structure to be consistent with the electron diffraction data. However, at the HF level the *C*₂ conformer is only 0.04 kcal mol⁻¹ above the *C*₁ conformer. The inclusion of zero-point energy corrections for the two conformers increased this to 0.16 kcal mol⁻¹. However, both of these are substantially lower than the *C*₃ and *D*₃ conformations. At the MP2 level the energies of *C*₂ and *C*₁ are reversed with *C*₂ now 0.23 kcal mol⁻¹ lower than the *C*₁. Both are still substantially lower in energy than the other two conformers. Also given in Table 5 are the vertical ionization energies in electronvolts computed as the difference between the energies of the parents and the ions with identical atom positions. These were used in combination with the calculated orbital energies to suggest approximate computed photoelectron spectra (7–14 eV) for each of the four conformers. These are depicted as vertical lines in Figure 2 for comparison with the experimental photoelectron spectrum.

TABLE 4: Comparison of X-ray Structure of [9]aneS₃ and MP2/6-31G* Calculated Geometries

bond/angle ^a	X-ray ^b	<i>C</i> ₃	<i>C</i> ₁	<i>C</i> ₂	<i>D</i> ₃
S1–C2	1.820(5)	1.8163	1.8207	1.8177	1.8202
C2–C3	1.510(6)	1.5307	1.5272	1.5233	1.5362
C3–S4	1.823(5)	1.8151	1.8145	1.8173	1.8202
S4–C5	1.820(5)	1.8163	1.8295	1.8202	1.8202
C5–C6	1.510(6)	1.5307	1.5302	1.5349	1.5362
C6–S7	1.823(5)	1.8151	1.8162	1.8202	1.8202
S7–C8	1.820(5)	1.8163	1.8190	1.8173	1.8202
C8–C9	1.510(6)	1.5307	1.5270	1.8177	1.5362
S1–C2–C3	113.0(4)	113.66	114.45	117.50	114.54
C2–C3–S4	117.0(4)	117.66	115.68	118.03	114.54
C3–S4–C5	102.8(3)	101.51	103.37	103.25	100.26
S4–C5–C6	113.0(4)	113.66	112.28	116.53	114.54
C5–C6–S7	117.0(4)	117.66	117.37	116.53	114.54
C6–S7–C8	102.8(3)	101.51	103.64	103.25	100.26
C7–C8–C9	113.0(4)	113.66	113.04	118.03	114.54
S1–C2–C3–S4	58.5	55.54	73.49	-66.42	-142.79
C2–C3–S4–C5	55.1	58.16	-88.77	-61.38	61.13
C3–S4–C5–C6	-131.1	-130.36	133.31	105.25	61.13
S4–C5–C6–S7	58.5	55.54	-91.28	-84.93	-142.79
C5–C6–S7–C8	55.1	58.16	66.56	105.25	61.13
C6–S7–C8–C9	-131.1	-130.37	-116.84	-61.38	61.13

^a Bond lengths in angstroms, and angles in degrees. ^b Experimental data from ref 3. Values in parentheses are estimated errors (1s) in the last digit quoted.

TABLE 5: Calculated Energies for [9]aneS₃ Conformations at the HF and MP2 Levels of Theory and Vertical Ionization Energies^a

conformer	neutral molecule		vertical ion	
	HF/6-31G* (kcal mol ⁻¹)	MP2/6-31G* (kcal mol ⁻¹)	HF/6-31G* (eV)	MP2/6-31G* (eV)
<i>C</i> ₁	0.00 ^b	0.23	7.56	8.18 ^c
<i>C</i> ₂	0.05	0.00 ^d	8.26	8.07
<i>C</i> ₃	5.14	4.25	7.29	7.90 ^c
<i>D</i> ₃	2.52	1.90	7.86	8.46

^a Zero-point energies corrections are not included. ^b Lowest energy: -1426.711 666 4 au. ^c Adiabatic ionizations were also calculated for these ions at the MP2/6-31G* level and were found to be 8.08 and 7.46 eV for the *C*₁ and *C*₃ conformations. ^d Lowest energy: -1427.869 766 6 au.

Microwave Studies. Listed in Table 6 are the experimental rotational constants and the rotational constants given by the optimized parameters for the four structures. The three *C* symmetry structures have dipole moments along various axes and thus would be expected to have microwave spectra. The absence of a dipole moment for the symmetric *D*₃ structure precludes investigation by conventional microwave spectroscopy. Rigid rotor microwave spectra for each of the other structures were calculated from the rotational constants and dipole moments which are given in Table 6. The *C*₁ theoretical microwave spectrum was found to allow reasonable assignments to most of the measured microwave transitions and is shown along with the experimental microwave spectrum in Figure 4. The assignment of the microwave spectrum to the *C*₁ structure is supported by the agreement between measured and calculated rotational constants and the observation of strong “a” dipole type transitions in the spectrum. The *C*₁ conformation’s theoretical structure is expected to have a strong “a” dipole and a slightly weaker “c” dipole moment.

Photoelectron Spectroscopy. The He I photoelectron spectrum of the valence region of 1,4,7-trithiacyclononane is shown in Figure 1. This is very similar to the spectrum previously reported.^{4–6} The ionizations in the region from 8 to 10 eV arise from ejection of an electron from sulfur 3p lone-pair orbitals, while those from about 10–12 eV corresponds to removal of an electron from S–C σ bonding orbitals. Ionizations observed

TABLE 6: Rotational Constants from the Least-Squares Structure Fit to the Experimental Spectrum Followed by Calculated Rotational Constants for the MP2 Minimized Structures

conformer	A (MHz)	B (MHz)	C (MHz)	μ_a (D)	μ_b (D)	μ_c (D)
expt (C_1) ^a	1155.651(3)	998.442(3)	629.426(2)	yes	no	yes
C_1	1157.18	994.96	630.16	1.4398	0.1758	0.9483
C_2	1066.85	1063.16	656.06	1.6400	0.0344	0.0001
C_3	1093.54	1093.42	639.89	0.0000	0.0000	4.2961
D_3	1009.95	1009.95	547.79	0.0000	0.0000	0.0001

^a The standard deviations on these numbers represent 2σ from the three parameter fit to the spectrum. The standard deviation of this fit was $\sigma = 33$ kHz.

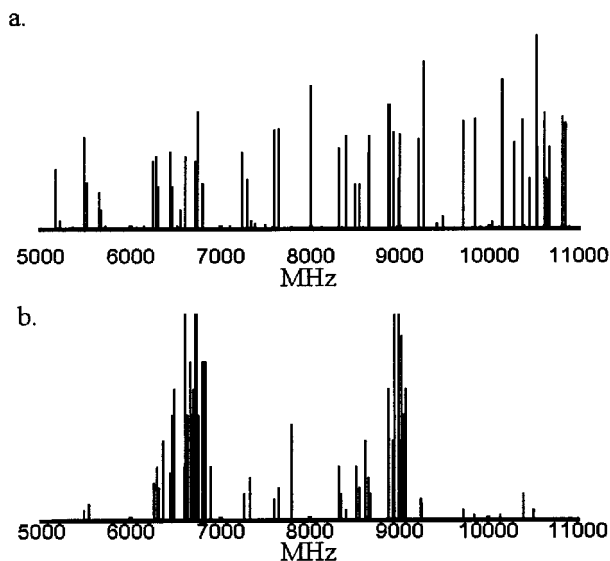


Figure 4. (a) Microwave spectrum for the calculated C_1 symmetry structure of [9]aneS₃ with “a” and “c” dipole moments. (b) Experimental microwave spectrum of [9]aneS₃ (see Table 2 for list of transitions).

at lower energies correspond to removal of electrons from the C–C σ and C–H σ bonding orbitals.

The gas-phase conformation of 1,4,7-trithiacyclononane was previously assigned as a conformation of C_3 symmetry based on the observed splitting of the S lone-pair ionizations into a 2:1 pattern.⁴ The new, high-resolution data indicate that the previously identified sulfur MO doublet of ratio 2:1 is actually made up of two or more sets of peaks that overlap in this region. The expansion of this region in Figure 2 shows additional structure. In addition, these ionization bands are much broader than typically observed for S lone-pair ionizations,²⁵ indicating that more than two S lone-pair ionizations are actually observed in this region. Also included in Figure 2 is an analytical representation of the spectrum in terms of asymmetric Gaussians. (Details are given in the Experimental Section.) The spectrum contains at least four discrete ionizations. Since any individual conformation of 1,4,7-trithiacyclononane can give at most three sulfur lone-pair ionizations, observation of four indicates that at least two conformations must be present in the gas phase. This is in conformity with both the electron diffraction study reported before¹² and microwave results reported here.

The calculated sulfur lone-pair orbital energies for the two conformations observed in the microwave spectra are also shown in Figure 2 plotted as lines. All of the orbital energies were shifted by -0.2 eV to make the calculated HOMO energies agree with the observed first vertical ionization energy. The solid lines represent the calculated orbital energies for the C_1 conformation, while the dashed lines represent the calculated orbital energies for the C_2 conformation. The calculated orbital energy separations are in excellent agreement with the photoelectron spectrum, providing further evidence that both the C_1 and C_2 conformations are present in the gas phase.

Microwave Spectroscopy. Measured transition frequencies along with the quantum number assignments for [9]aneS₃ are listed in Table 2. This table includes the 40 transitions which match up with those predicted (to within 0.4%) for the C_1 asymmetric top rigid rotor spectrum. In Figure 4 the predicted and experimental C_1 spectrum are shown. On the basis of the excellent agreement between the spectra, an assignment of C_1 symmetry is made. The molecular parameters of the spectral line fittings are shown in Table 6. The assignments from this predicted C_1 spectrum produced a spectral fit with a standard deviation of 33 kHz, which is higher than the normal uncertainty of 1–20 kHz often found in rigid molecules. The rotational constants found by this spectral fit are in excellent agreement with the calculated values for the C_1 conformation reported in Table 6. Both “a” and “c” dipole assignments were made, and the calculations indicate the presence of a weak “b” dipole. However, there was no experimental evidence for the “b” dipole transitions.

The importance of inversion and pseudorotation to the spectra of [9]aneS₃ conformers is not known. There has been success fitting the data to a rigid asymmetric structure, but this alone does not explain the existence of 21 additional lines (listed in Table 3) in the same frequency range. The PES data indicate it is likely that at least more than one structure is present in the gas phase. If there is another asymmetric structure it may account for many of these lines. Assignment of the extra lines to the present (C_1) data fit increases the standard deviations to greater than 1 MHz.

The calculated results for the C_1 conformer led to sufficiently good agreement with the microwave spectrum; it was of interest to consider the implications of the other structural results. Of course, the D_3 structure cannot be ruled out by microwave techniques since a lack of a dipole moment would render it invisible to the microwave radiation. However, the C_3 conformation should give a simple symmetric top spectrum in which two separate transitions fall in the range of the microwave spectrum scanned. For these levels $J' \leftarrow J = 3 \leftarrow 2$ and $4 \leftarrow 3$ the ratio of frequencies for these two transitions would have to be near $6B/8B = 0.75$. Since none of the measured lines fulfill this requirement, it seems unlikely that the C_3 conformation is present in sufficient amount to be detected by the spectrometer.

The C_2 structure is predicted from the calculations to have a strong “a” dipole moment. Its presence should be clear in the microwave spectrum and as an asymmetric top would account for a multitude of transitions in the region scanned. Several spectral fits were attempted using assignments from the calculated rotational constants in addition to assignments made by reasonable judgment. A few assignments gave reasonable spectral fits on the order of 1 MHz accuracy, but the constants found in these fits predicted more microwave transitions in regions where there were none. One of these assignments yielded a five-line ($\sigma = 25$ kHz) fit with rotational constants that were within 2% of those predicted for the C_2 structure. However, the combined assignments for both sets of rotational

constants still did not explain additional lines in the spectrum, and the other strong lines that were predicted did not appear. Thus, a C_2 assignment is still unsubstantiated. It appears from analysis of the microwave data that there may be another asymmetric structure (C_2 or C_1) that accounts for the excess lines of the C_1 spectral fit. If the barrier to internal motion is very low for this conformer, it could be extremely difficult to interpret the microwave spectrum. Perhaps there are large-amplitude internal motions that split the rotational energy levels into the complex patterns observed in Figure 4. Nonrigid behavior with a higher barrier also could account for the frequency deviations observed for the C_1 conformer.

Discussion

The conformation of [9]aneS₃ in the gas phase was originally assigned on the basis of its photoelectron spectrum.⁴ Two ionization peaks exhibited a 2:1 ratio and a large separation in the range for the sulfur 3p lone pair. This was consistent with the semiempirical MO energies of the C_3 conformer, suggesting that the gas-phase and solid-state conformations were identical. However, improved resolution shows at least four ionizations and more than one conformation. The ab initio results provide a compelling analysis of the high-resolution photoelectron spectrum. A composite of the conformations with C_1 and C_2 symmetry with little or no presence of conformations of higher symmetry provide an excellent fit of the spectrum. Microwave spectroscopy, in principle, can provide an unequivocal analysis in the gas phase of the conformations with dipole moments. However, analysis of cyclic molecules by microwave spectroscopy has been successfully accomplished only for the smallest or most symmetric (mainly planar) rings.²⁶ Only a limited number of nonplanar rings have been successfully analyzed. Ring puckering has been studied in four-membered rings, and pseudorotation has been modeled for larger rings. In these nonplanar rings the spectral complexity arising from low-energy internal motions generally makes microwave spectral analyses more difficult. However, ring molecules with dipole moments will generally exhibit microwave spectra. Thus, measuring the spectra of these molecules is straightforward, but the interpretation of the data can be a problem. Many nonplanar ring systems have the ability to change conformation rapidly such that the rigid rotor assumption is no longer valid. Generally, one has to introduce extra potential energy terms into the Hamiltonian for a complete treatment of these systems. The normal distortion parameters included in microwave spectral fits do not directly apply since these account for centrifugal forces occurring during rotation of the molecule, whereas pseudorotation and inversion must be treated more like a vibration. Inversion or internal motion generally leads to splitting and shifting of the microwave transitions. Nevertheless, as shown in this paper fitting the C_1 structure obtained by theoretical calculations to the microwave spectrum confirms the presence of the C_1 structure, but its rigidity is still questionable. Attempts to fit the C_2 structure obtained by theoretical calculations with the microwave data are less convincing but supportive. Thus, the data obtained by all three methods unequivocally show that there is more than one conformer of [9]aneS₃ in the gas phase. One of these is shown to be the C_1 conformer and the other major conformer is likely to be the C_2 conformer. No evidence is obtained for significantly populating the C_3 conformer.

Acknowledgment. R.S.G. gratefully acknowledges support of this work by the National Science Foundation (CHE-9422200). M.B. gratefully acknowledges the National Science Foundation for partial support in the purchase of the IBM workstations used in the study. S.G.K. gratefully acknowledges support of this work by the National Science Foundation (CHE-9634130). Construction of the pulsed-beam spectrometer was also supported by the NSF. S.G.K. also acknowledges the support of the Petroleum Research Fund, administered by the American Chemical Society, for partial support of this research. J.F.M. was supported by a Research Corporation, "Partners in Science" award. The authors thank Dr. Yunqi Liu for purifying the [9]aneS₃.

References and Notes

- (1) Cooper, S. R.; Rawle, S. C. *Struct. Bonding (Berlin)* **1989**, 72, 1.
- (2) Blake, A. J.; Schröder, M. In *Advances in Inorganic Chemistry*; Sykes, A. G., Ed.; Academic Press: New York, 1990; Vol. 35, p 1.
- (3) Glass, R. S.; Wilson, G. S.; Setzer, W. N. *J. Am. Chem. Soc.* **1980**, 102, 5068.
- (4) Setzer, W. N.; Coleman, B. R.; Wilson, G. S.; Glass, R. S. *Tetrahedron* **1981**, 37, 2743.
- (5) Novak, I.; Ng, S. C.; Potts, A. W. *Spectrochim. Acta* **1994**, 50A, 353.
- (6) Durrant, M. C.; Richards, R. L.; Firth, S. *J. Chem. Soc., Perkin Trans. 2* **1993**, 445.
- (7) Setzer, W. N.; Glass, R. S. In *Conformational Analysis of Medium-Sized Heterocycles*, Glass, R. S., Ed.; VCH Publishers: New York, 1988; p 151.
- (8) Beech, J.; Cragg, P. J.; Drew, M. G. B. *J. Chem. Soc., Dalton Trans.* **1994**, 719.
- (9) Blake, A. J.; Gould, R. O.; Greig, J. A.; Holder, A. J.; Hyde, T. I.; Schröder, M. *J. Chem. Soc., Chem. Commun.* **1989**, 876.
- (10) Clarkson, J. A.; Yagbasan, R.; Blower, P. J.; Cooper, S. R. *J. Chem. Soc., Chem. Commun.* **1989**, 1244.
- (11) Sanaullah; Kano, K.; Glass, R. S.; Wilson, G. S. *J. Am. Chem. Soc.* **1993**, 115, 592.
- (12) Blom, R.; Rankin, D. W. H.; Robertson, H. E.; Schröder, M.; Taylor, A. *J. Chem. Soc., Perkin Trans. 2* **1991**, 773.
- (13) Lockhart, J. C.; Tomkinson, N. P. *J. Chem. Soc., Perkin Trans. 2* **1992**, 533.
- (14) Park, Y. S.; Shurvell, H. F. *J. Mol. Struct.* **1996**, 378, 165.
- (15) Gaussian 94, Revision B.3: Frisch, M. J.; Trucks, G. W.; Schlegel, H. B.; Gill, P. M. W.; Johnson, B. G.; Robb, M. A.; Cheeseman, J. R.; Keith, T.; Petersson, G. A.; Montgomery, A. J.; Raghavachari, K.; Al-Laham, M. A.; Zakrzewski, V. G.; Ortiz, J. V.; Foresman, J. B.; Peng, C. Y.; Ayala, P. Y.; Chen, W.; Wong, M. W.; Andres, J. L.; Replogle, E. S.; Gomperts, R.; Martin, R. L.; Fox, D. J.; Binkley, J. S.; Defrees, D. J.; Baker, J.; Stewart, J. P.; Head-Gordon, M.; Gonzalez, C.; and Pople, J. A. Gaussian, Inc., Pittsburgh, PA, 1995.
- (16) Möller, C.; Plesset, M. S. *Phys. Rev.* **1934**, 46, 618.
- (17) Hehre, W. J.; Ditchfield, R.; Pople, J. A. *J. Chem. Phys.* **1972**, 56, 2257.
- (18) Lichtenberger, D. L.; Kellogg, G. E.; Kristofzski, J. G.; Page, D.; Turner, S.; Klinger, G.; Lorenzen, J. *Rev. Sci. Instrum.* **1986**, 57, 2366.
- (19) Jatcko, M. E. Ph.D. Dissertation, University of Arizona, 1990.
- (20) Renshaw, S. K. Ph.D. Dissertation, University of Arizona, 1991.
- (21) The He I β line is a secondary wavelength emitted by the He discharge source that causes a "shadow spectrum" shifted by 1.9 eV and ~3% of the intensity of the He I α spectrum. Rabalais, J. W. *Principles of Ultraviolet Photoelectron Spectroscopy*; Wiley-Interscience: New York, 1977; p 23.
- (22) Lichtenberger, D. L.; Copenhaver, A. S. *J. Electron Spectrosc. Relat. Phenom.* **1990**, 50, 335.
- (23) Bumgarner, R. E.; Kukolich, S. G. *J. Chem. Phys.* **1987**, 86, 1083.
- (24) Anet, F. A. L. *J. Am. Chem. Soc.* **1990**, 112, 7172.
- (25) For examples see the other spectra in ref 4: Kimura, K.; Katsumata, S.; Achiba, Y.; Yamazaki, T.; Iwata, S. *Handbook of He I Photoelectron Spectra of Fundamental Organic Molecules*; Japan Scientific Societies Press: Tokyo, 1981.
- (26) Kroto, H. W. *Molecular Rotation Spectra*; Dover Publications Inc.: New York, 1992; p 220.